Processing and Application of Ceramics 15 [3] (2021) 314–318
https://doi.org/10.2298/PAC2103314C

Short communication

Novel yellow to blackish green Ni-doped aluminium titanate ceramic pigments

Junhua Chen[1], Li Yin[1], Guo Feng[1,2,*], Feng Jiang[1,*], Qianqian Zhao[1], Shanfang Lan[1], Xiaojun Zhang[1], Feifei Zhong[1], Jianmin Liu[2], Qing Hu[1], Weihui Jiang[1,2,*]

[1]*Department of Material Science and Engineering, Jingdezhen Ceramic Institute, Jingdezhen 333000, China*
[2]*National Engineering Research Center for Domestic & Building Ceramics, Jingdezhen Ceramic Institute, Jingdezhen 333000, China*

Received 29 April 2021; Received in revised form 29 August 2021; Accepted 4 September 2021

Abstract

Novel yellow to blackish green Ni-doped aluminium titanate (Al_2TiO_5) ceramic pigments were synthesized by solid-state reaction method at 1400 °C. Effects of nickel doping content on phase composition, microstructure, optical properties and stability were studied. The results show that the higher content of Al_2TiO_5 phase and the reduction of the lattice distortion of aluminium titanate could be attributed to the entry of nickel ions into aluminium titanate lattice resulting in the formation of solid solution. Ni-doped aluminium titanate ceramic pigments show exceptional glaze colouring and are expected to be promising high-temperature pigments.

Keywords: *pigments, aluminium titanate, Ni-doping, structure, optical properties*

I. Introduction

The inorganic pigments are widely used in paint, plastics, glazes and ceramics due to their thermal stability, chemical stability and high tinting strength [1,2]. The ceramic pigment is a kind of decorative material used for the painting of ceramic products [3,4]. It can be divided into tin-based [5], zirconium-based [6], spinel-type [7], rutile-type [8], corundum-type [9] and encapsulated ceramic pigments [10]. It can also be divided into high-temperature and low-temperature pigments. There are many kinds of low-temperature pigments and relatively few pigments with high stability at high temperature, especially with the temperature higher than 1300 °C [11].

Aluminium titanate (Al_2TiO_5) has the characteristics of high melting point (1860 °C) and high corrosion resistance to alkali, salt and glass melt [12]. Compared with spinel, corundum and rutile types of pigments, aluminium titanate base ceramic pigment has better corrosion resistance to glass melt and high temperature stability. Also, compared with zirconia and tin based ceramic pigments, aluminium titanate ceramic pigment contains two doping positions of trivalent aluminium ion and tetravalent titanium ion, which can be adapted to different colouring ions. It also has a wider range of high concentration doping (high colouring effect) feasibility. At present, the research on aluminium titanate base ceramic pigment has just started. Michele *et al.* [13] prepared M doped Al_2TiO_5 solid solution ceramic pigments (where M is Cr (green colour), Mn (brown colour), Co (pink colour)) by solid-phase reaction method at 1400 °C.

With the dimethyl sulfoxide-d^6 (DMSO-d^6) transition occurring in the visible light region, some transition metal oxides show interesting hues and properties and are attracting focus of the researchers as new pigments. For decades, several inorganic pigments which contain heavy metals and transition metals have been extensively used for industrial and commercial purposes [14]. Several transition metal oxides undergo energetic transitions in the visible region that produce interesting colours and good performance and have thus attracted attention as novel chromophores [15]. Ni-doping is

* Corresponding author: tel: +86 798 8499328,
e-mail: *jiangfeng@jci.edu.cn* (Feng Jiang)
jiangweihui@jci.edu.cn (Weihui Jiang)
fengguo@jci.edu.cn (Guo Feng)

expected to confer a rich colour to ceramic pigments via the $4s^2 3d^8$ ion configuration [16]. In this work, a novel Ni-doped Al_2TiO_5 emerald green ceramic pigment was developed. Effect of the Ni-doping concentration on the pigment performance was investigated.

II. Experimental

2.1. Preparation method

TiO_2 (analytically pure, AR), Al_2O_3 (analytically pure, AR) and Ni_2O_3 (analytically pure, AR) were used as starting materials directly without further refinement. TiO_2 and Al_2O_3 were weighed according to the stoichiometric ratio of aluminium titanate and placed in the mortar. Ni_2O_3 was weighed according to the doping content (5, 10, 15, 20 and 25 mol%) and the benchmark of aluminium titanate. The mixture was evenly mixed by grounding for 30 min. Finally, the samples were maintained at 1400 °C for 2 h. The samples were marked as W (without Ni-doping), A (5 mol%), B (10 mol%), C (15 mol%), D (20 mol%) and E (25 mol%).

The ceramic body and glaze were supplied by Peiyintang Ceramic Glaze Shop in Jingdezhen, China. The glazing process was performed by mixing the synthesized pigments with a transparent glaze (using mass ratio 6 to 94, respectively), followed by firing in air at 1200 °C for 2 h. In addition, the stability test of the samples is carried out for the selected samples W and D undergoing additional heat treatment at 1200 °C for 2 h.

2.2. Characterization

The crystal phase composition, crystal structure and crystal parameters of the samples were analysed by D8 type X-ray diffractometer. Step scanning method was used and CuKα target with the wavelength of $\lambda = 0.154$ nm was employed as the radiation source. The scanning ranges were from 10 to 70°. The crystal cell parameters were determined by the Rietveld refinement. Since the prepared samples consisted of different phases, the content of aluminium titanate under different process conditions was determined by the adiabatic method (self-cleaning method) for semi-quantitatively calculation of the content of each crystal phase. The *RIR*(*K*) coordinate of each phase can be checked through the PDF card (the coordinate of aluminium titanate phase the *RIR* value is 2, the *RIR* value of the rutile phase is 3.4 and the *RIR* value of the corundum phase is 1). The diffraction intensity of each phase was measured and the mass fraction of the required phase can be calculated [17,18]:

$$W_{Al_2TiO_5} = \frac{1}{\frac{K_{Al_2TiO_5}}{I_{Al_2TiO_5}} \cdot \sum_{i=1}^{n} \frac{I_i}{K_i}} \quad (1)$$

n is the number of phases to be measured and i is the phase to be measured.

Microstructure characterization of the powders was carried out by scanning electron microscopy (SEM, JSM-6700F). High-resolution transmission electron microscopy (HR-TEM) images were taken on a JEM-2010 microscope. In this experiment, the particle size and distribution of the samples were determined by a Mastersizer 3000 dynamic light scattering laser particle size analyser from Malvern, UK, where D_{10}, D_{50} and D_{90} represent the particle sizes corresponding to a cumulative particle size distribution of 10%, 50% and 90%, respectively. The WSD-3C full-automatic whiteness meter of Beijing Coroptics Instrument Company Limited was used to characterize the pigments. The conditions were set according to the table standard of The International Commission on Lighting (CIE).

III. Results and discussion

3.1. Structure and optical properties

Figure 1 shows the XRD patterns of the pigment samples with different nickel doping amounts of 5, 10, 15, 20 and 25 mol%. Figure 1 also lists the XRD pattern of the sample without nickel doping. It can be seen from Fig. 1 that the first and second main crystal phases of the undoped sample are corundum and rutile, respectively, with only 20.64% of aluminium titanate phase. The aluminium titanate phase changes to be the second main crystal phase with the content of 43.14% when the nickel-doping amount is 5 mol%. The aluminium titanate phase changes to be the first main crystal phase with the content of 85.85%, 90.99%, 80.91% and 81.39% when the nickel doping amounts are 10, 15, 20 and 25 mol%, respectively. The aluminium titanate content decreases when the nickel doping amount increases to 20 and 25 mol%, indicating that too much nickel doping also affects the synthesis of aluminium titanate. Also, partial enlargement ($25.5° < 2\theta < 27°$) of XRD patterns on the right part of Fig. 1 show that the nickel-doped samples of aluminium titanate exhibit peaks shifting towards lower angles, indicating that

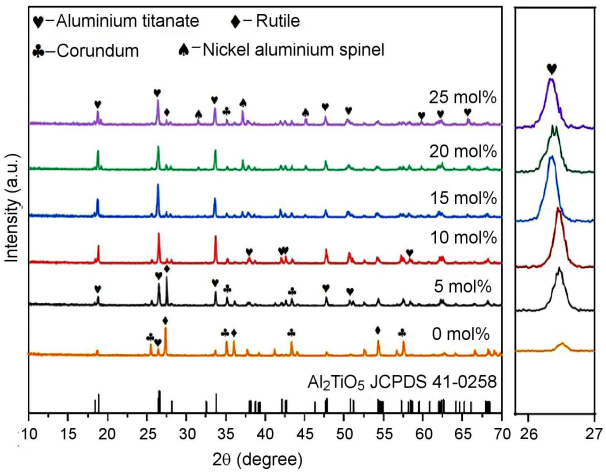

Figure 1. XRD patterns of samples with different Ni_2O_3 doping contents heat-treated at 1400 °C

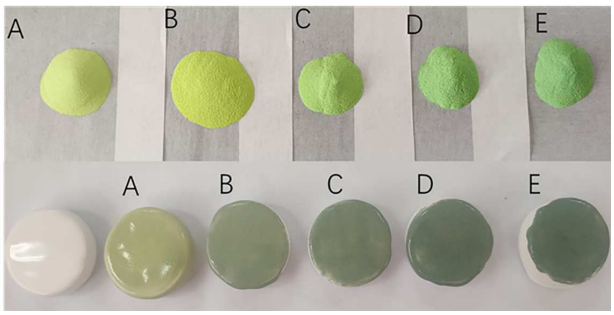

Figure 2. Samples of pigments with different Ni_2O_3 doping contents and their corresponding glazes

Table 1. Chromaticity values of pigments with different nickel doping contents

Sample	L^*	a^*	b^*
A - 5 mol%	73.96	−16.96	40.58
B - 10 mol%	69.59	−15.76	33.34
C - 15 mol%	62.02	−19.24	29.57
D - 20 mol%	58.07	−22.03	24.25
E - 25 mol%	56.54	−21.25	20.46

nickel has been incorporated into the aluminium titanate lattice with the formation of solid solution. Thus, nickel doping can promote mass transfer and the formation of aluminium titanate.

Figure 2 shows the picture of aluminium titanate base ceramic pigments and their corresponding glazes with different nickel doping amounts. The pigments change from yellow to blackish green with the increasing nickel doping amounts from 5 to 25 mol%. This is because with the increase of Ni_2O_3 content, more nickel enters into the crystal lattice of Al_2TiO_5. Table 1 lists the L^*, a^*, b^* chroma values of the samples with different nickel doping amounts. L^* and b^* values of the pigments decline from 73.69 to 56.54, and from 40.58 to 20 with the nickel doping amount increase. The pigments change from yellow to blackish green.

The wide pigments colouring range is mainly ascribed to the outer electronic structure of nickel ion ($4s^2 3d^8$). The outermost electronic structure is unstable with easy transition between layers. If ΔE of track transition from ground state E_1 to excited state E_2 ($\Delta E = E_2 - E_1$) is in the visible light wave energy range, there will be a corresponding wave absorption of monochromatic light which can be affected by the coordination number at the same time. Therefore, the nickel doping of the aluminium titanate pigments change their colour from yellow to blackish green.

Figure 3 shows the SEM, TEM and laser particle size distribution test results of the sample C with 15 mol% Ni-doping content prepared under the optimal conditions. These results are highly consistent in particle size. SEM and TEM graphs show that the sample particles are irregular in shape, with dense surface and excellent dispersion and main particle size in the range from 2 to 5 μm. Meanwhile, according to the laser particle size distribution graph shown in Fig. 3c, the D_{50} of the sample C is 2.78 μm. The particles are mainly distributed in a narrow range of 0.905 μm to 4.56 μm, and the most probable particle size is 3.58 μm. The laser particle size distribution is consistent with the SEM and TEM measurement. These results indicate that the Ni-doped aluminium titanate pigments could have broad applications such as glazing.

3.2. *Pigment stability*

To test the stability of aluminium titanate ceramic pigment, the glaze sample W without nickel doping and the sample D with nickel doping content of 20 mol% were chosen to hold at 1200 °C for 2 h. Figure 4 shows the XRD patterns of the samples after the stability test analysis (W-1200 and D-1200 are samples without nickel doping and 20 mol% nickel doping after stability test). For comparison, Fig. 4 also shows the XRD pattern of the sample D-1400 which corresponds to the pigment D-1200 before stability test. The aluminium titanate phase synthesized in the sample without nickel doping has completely decomposed into corundum and rutile phases, which is because of the instability of aluminium titanate at medium temperature (800–1280 °C). Although corundum and rutile phases also increase in the sample D with 20 mol% nickel doping content, the aluminium titanate phase content in the sample D-1200 does not significantly decrease compared with

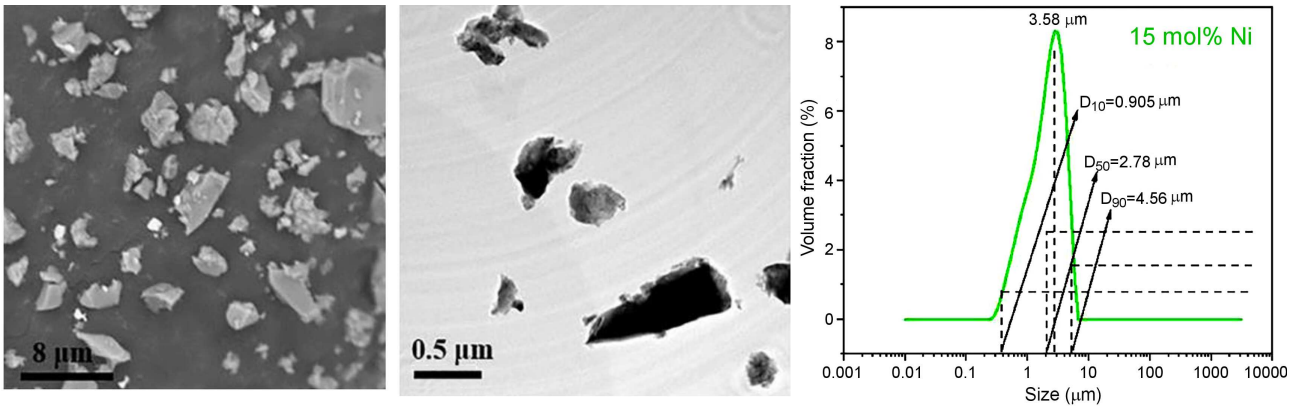

Figure 3. SEM (a), TEM (b) and particle size distribution curves (c) of nickel-doped aluminium titanate-based ceramic pigments prepared under the optimal conditions

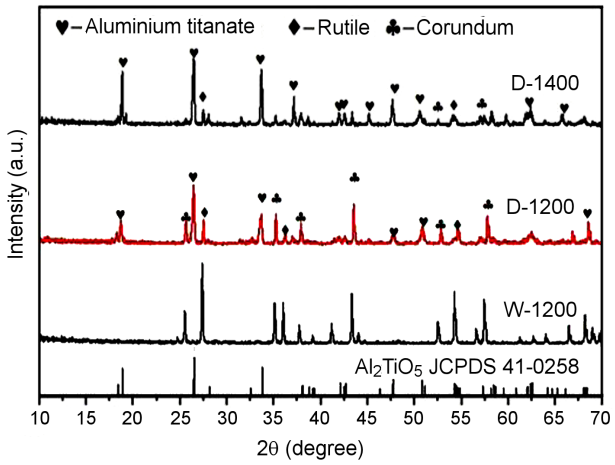

Figure 4. XRD patterns of samples W-1200, D-1400 and D-1200

the 80.91% in the original sample D-1400 before stability test.

To confirm the cause of stability difference between the sample without nickel doping and the sample D, the lattice constants of these two samples were calculated by adiabatic method. The lattice constants of aluminium titanate phase in the sample W without nickel doping are a = 9.44675 Å, b = 9.60339 Å and c = 3.59107 Å. The lattice constants of aluminium titanate phase in the sample D are a = 9.5290 Å, b = 9.6654 Å and c = 3.59107 Å. For comparison, a and b increase significantly and c is roughly the same. This is because the nickel ions have entered the aluminium titanate lattice at A-site replacing Al^{3+} ions. Ni^{3+} has ionic radius of 74 pm and Al^{3+} has 67.5 pm. According to the ion size effect, since the ratio of the radius size difference is 8%, which is less than 15%, a continuous solid solution can be formed. The volume of the lattice is increased with nickel addition, i.e. a and b axes are increased. Meanwhile, aluminium titanate crystal unit is composed of [AlO_6] and [TiO_6] octahedron coordinated by Al^{3+}, Ti^{4+} and O^{2-}. [AlO_6] is more prone to be distorted than [TiO_6], which is also an important reason why aluminium titanate is easy to decompose at 750–1280 °C. The valence state of Ni ions is +3 which is closer to Al^{3+}. The Ni^{3+} ions in the system will replace the unstable Al^{3+} ions, which reduces the lattice distortion degree and thus improves the thermal stability of aluminium titanate. Therefore, the nickel-doping stabilizes the crystal structure of aluminium titanate and improves the thermal stability of aluminium titanate.

IV. Conclusions

Novel yellow to blackish green Ni-doped aluminium titanate ceramic pigments were synthesized by solid-state reaction method. It is discovered that appropriate nickel doping content not only promotes the formation of aluminium titanate, but also stabilizes it. This is because nickel ions have been doped into the lattice of aluminium titanate and thus reduce its lattice distortion degree. Ni-doped aluminium titanate pigments have a broad market prospect.

Acknowledgements: This work was supported by the National Natural Science Foundation of China [grant numbers 52072162, 51962014]; Jiangxi Provincial Natural Science Foundation [grant numbers 20202ACBL214006, 20202ACBL214008, 20192BBEL50022, 2020ZDI03004, 20202BABL214013]; Open fund project of the Key Laboratory of Inorganic Coating Materials, Chinese Academy of Science (ICM-202001); the Jingdezhen science and technology plan project (20202GYZD013-09, 20202GYZD013-14); the Science Foundation of Jiangxi Provincial Department of Education (GJJ201324, GJJ201345).

References

1. B. Bae, Wendusu, S. Tamura, N. Imanaka, "Novel environmentally friendly inorganic yellow pigments based on gehlenite-type structure", *Ceram. Int.*, **42** [13] (2016) 15104–15106.
2. P. Luňáková, M. Trojan, J. Luxová, J. Trojan, "$BaSn_{1-x}Tb_xO_3$: A new yellow pigment based on a perovskite structure", *Dyes Pigments*, **96** [1] (2013) 264–268.
3. J. Calbo, A. Mestre, A. Garcia, M.A. Tena, M. Llusar, G. Monros, "Multicomponent black coloured spinels from alkoxides", *J. Sol-Gel Sci. Technol.*, **26** [1-3] (2003) 191–194.
4. M. Llusar, A. Forés, J.A. Badenes, J. Calbo, M.A. Tena, G. Monrós, "Colour analysis of some cobalt-based blue pigments", *J. Eur. Ceram. Soc.*, **21** [8] (2001) 1121–1130.
5. H.R.C. Ricardo, J. Rufner, P. Hidalgo, D. Gouvêa, A.C.H. Joséa, K. Benthem, "Surface segregation in chromium-doped nanocrystalline tin dioxide pigments", *J. Am. Ceram. Soc.*, **95** [1] (2012) 170–176.
6. J.M. Calatayud, J. Alarcón, "V-containing ZrO_2 inorganic yellow nano-pigments prepared by hydrothermal approach", *Dyes Pigments*, **146** (2017) 178–188.
7. R. Guo, Q. Wang, J. Bao, X. Song, "Preparation and properties of Co-doped magnesium lanthanum hexaluminat blue ceramics", *Ceramics*, **3** (2020) 235–244.
8. J. Večeřa, J. Čech, P. Mikulášek, P. Šulcová, "The study of rutile pigments $Ti_{1-3x}Cr_xM_{2x}O_2$", *J. Eur. Ceram. Soc.*, **11** [9] (2013) 1447–1455.
9. M. Kato, M. Takahashi, H. Unuma, S. Suzuki, "Synthesis of reddish pink pigment by addition of Mg^{2+} into $(Al,Cr)_2O_3$ corundum", *J. Ceram. Soc. Jpn.*, **107** [1024] (2010) 181–183.
10. Q. Chang, X. Wang, Y. Wang, Q. Bao, J. Zhou, Q. Zhu, "Encapsulated carbon black prepared by sol-gel-spraying: A new black ceramic pigment", *J. Eur. Ceram. Soc.*, **34** [13] (2014) 3151–3157.
11. G. Monros, *Pigment, Ceramic, Encyclopedia of Color Science and Technology*, Springer, New York, 2013.
12. A. Mahandrimanana, R.J.P. Corriu, L. Dominique, M.P. Hubert, V. Andre, "Nonhydrolytic sol-gel process: Aluminium and zirconium titanate gels", *J. Sol-Gel Sci. Technol.*, **8** [1-3] (1997) 89–93.
13. M. Dondi, T.S. Lyubenova, J.B. Carda, M. Ocaña, "M-

doped Al_2TiO_5 (M = Cr, Mn, Co) solid solutions and their use as ceramic pigments", *J. Am. Ceram. Soc.*, **92** [9] (2009) 1972–1980.
14. A. García, M. Llusar, J. Calbo, M.A. Tena, G. Monrós, "Low-toxicity red ceramic pigments for porcelainised stoneware from lanthanide-cerianite solid solutions", *Green Chem.*, **3** [5] (2001) 238–242.
15. Y. Ping, "Discussion on the relationship between the color and structure of ceramic pigments", *Chin. Ceram.*, **1** [6] (1998) 18–20.
16. M. Llusar, E. García, M.T. García, C. Gargori, J.A. Badenes, G. Monrós, "Synthesis, stability and coloring properties of yellow-orange pigments based on Ni-doped karrooite $(Ni,Mg)Ti_2O_5$", *J. Eur. Ceram. Soc.*, **35** [1] (2015) 357–376.
17. Y.H. Liu, P.A. Liu, *Principle and Application of X-ray Diffraction Analysis*, Chemical Industry Press, Beijing, 2003.
18. F.H. Chung, "Quantitative interpretation of X-ray diffraction patterns of mixtures. II. Adiabatic principle of X-ray diffraction analysis of mixtures", *J. Appl. Cryst.*, **7** (1974) 526–531.